APL Materials

Quasi-indirect measurement of electrocaloric temperature change in $PbSc_{0.5}Ta_{0.5}O_3$ via comparison of adiabatic and isothermal electrical polarization data

Cite as: APL Mater. **9**, 010701 (2021); https://doi.org/10.1063/5.0037809
Submitted: 16 November 2020 . Accepted: 23 December 2020 . Published Online: 19 January 2021

S. Crossley, R. W. Whatmore, N. D. Mathur, and X. Moya

APL Materials RESEARCH UPDATE scitation.org/journal/apm

Quasi-indirect measurement of electrocaloric temperature change in $PbSc_{0.5}Ta_{0.5}O_3$ via comparison of adiabatic and isothermal electrical polarization data

Cite as: APL Mater. 9, 010701 (2021); doi: 10.1063/5.0037809
Submitted: 16 November 2020 • Accepted: 23 December 2020 •
Published Online: 19 January 2021

View Online Export Citation CrossMark

S. Crossley,[1] R. W. Whatmore,[2] N. D. Mathur,[1,a)] and X. Moya[1,a)]

AFFILIATIONS

[1] Department of Materials Science, University of Cambridge, Cambridge CB3 0FS, United Kingdom
[2] Department of Materials, Royal School of Mines, South Kensington Campus, Imperial College London, London SW7 2AZ, United Kingdom

Note: This paper is part of the Special Topic on 100 Years of Ferroelectricity—A Celebration.
[a)] **Authors to whom correspondence should be addressed:** ndm12@cam.ac.uk and xm212@cam.ac.uk

ABSTRACT

Electrically driven adiabatic changes of temperature are identified in the archetypal electrocaloric material $PbSc_{0.5}Ta_{0.5}O_3$ by comparing isothermal changes of electrical polarization due to the slow variation of electric field and adiabatic changes of electrical polarization due to the fast variation of electric field. By obtaining isothermal (adiabatic) electrical polarization data at measurement (starting) temperatures separated by <0.4 K, we identify a maximum temperature change of ~2 K due to a maximum field change of 26 kV cm^{-1} for starting temperatures in the range of 300 K–315 K. These quasi-indirect measurements combine with their direct, indirect, and quasi-direct counterparts to complete the set and could find routine use in the future.

Voltage-driven thermal changes known as electrocaloric (EC) effects are maximized near phase transitions in ferroelectric materials[1,2] and can be used to pump heat in cooling cycles if the process is nominally reversible,[2] such that thermal changes and the concomitant changes of electrical polarization have equal magnitude on field application and field removal despite any field hysteresis. EC effects have now been exploited in a number of prototype cooling devices, where the flow of heat is driven by the temperature change that can be achieved in the working body under adiabatic conditions.[3–16] The EC behavior of a given material may be identified in terms of an adiabatic temperature change ΔT, an isothermal entropy change ΔS, or the corresponding isothermal heat Q. These parameters can be obtained via direct measurements of ΔT or Q, quasi-direct measurements of heat that most traditionally yield ΔS, and indirect measurements that most immediately yield ΔS from isothermal measurements of electrical polarization P vs electric field E (or ΔT from adiabatic measurements of P).[1,2,17] Noting that these parameters can be interconverted either crudely via $c|\Delta T| \sim T|\Delta S| = |Q|$ using some effective value of specific heat capacity $c(T,E)$[1] or more precisely by constructing detailed maps of $S(T,E)$ or $T(S,E)$ using $c(T,0)$ without requiring $c(T,E)$,[17–19] we complete here the set of EC measurement techniques by demonstrating quasi-indirect measurements that yield $|\Delta T|$.

Using a single sample of $PbSc_{0.5}Ta_{0.5}O_3$ (PST), we made fast adiabatic $P_{adi}(E)$ measurements at closely spaced values of zero-field temperature T_z and slow isothermal $P_{iso}(E)$ measurements at closely spaced values of measurement temperature T. For analysis, we use the outer branches of $P_{adi}(E)$ and $P_{iso}(E)$ in $E \geq 0$, which are similar (see Ref. 17) to the outer (inner) branches of unipolar cycles that would yield cooling (heating) in EC applications. Note that we performed bipolar rather than unipolar measurements here, as unipolar cycles must be accompanied by bipolar cycles in order to position unipolar plots on the polarization axis, such that the viable acquisition of unipolar cycles would shorten the measurement time for each

$P_{\mathrm{iso}}(E)$ branch in light of the 30 s measurement constraint discussed later.

Using these outer branches in $E \geq 0$, we identify the nominally reversible adiabatic temperature change between any two points in $P_{\mathrm{adi}}(E)$ as the temperature difference between the two $P_{\mathrm{iso}}(E)$ plots that intersect these points. Note that the method could be executed just as accurately using the measured $Q(V)$ data, without the geometrical normalization that results in a $P(E)$ dataset. However, the resulting $P(E)$ data are more familiar and easier to compare with the literature, and the comparative nature of the quasi-indirect method ensures the cancellation of any errors associated with the geometrical measurements.

Our method was inspired by an analogous study of magnetocaloric gadolinium,[20] and its application to EC materials, using much denser data, is novel. It is an indirect method given that we do not make direct measurements of electrically driven temperature change, but it is less indirect than the indirect method because we can identify $|\Delta T|$ without heat capacity data, without requiring knowledge of sample geometry, without thermodynamic analysis (not formally valid with hysteresis, not formally valid for relaxors), and without the resultant data processing that can amplify systematic errors and lead to artifacts. We therefore describe our method as quasi-indirect, which completes the set of measurements and avoids the unwelcome possibility of calling it a second type of quasi-direct method. However, our measurements of temperature (T and T_z) rather than electrically driven temperature change are reminiscent of the quasi-direct method,[21,22] where one measures thermally driven isofield heat instead of electrically driven heat.

Our PST sample was similar to ~400 μm-thick samples for which we have reported direct and indirect EC measurements.[17] Those samples and the present sample all came from the same master wafer, and they were thinned, mounted, and electroded in the same way. The present sample was 330 μm thick and possessed an area of 0.19 cm^2. The Pt bottom electrode was ubiquitous. The Pt top electrode fell ~0.5 mm from the sample edges, and its effective area was 0.11 cm^2 after incorporating a ~6% increase for fringing fields.[23] A smear of vacuum grease around the top electrode prevented arcing. While slowly varying measurement temperature T (starting temperature T_z) with a cryogenic probe that was fabricated in house,[24] we measured the isothermal (adiabatic) electrical polarization using a Radiant Precision Premier II with a trek high-voltage amplifier, which integrated the displacement current that resulted from the application of a continuous triangular driving waveform of magnitude 26 kV cm^{-1} and period 30 s (period 0.5 s). Sample temperature was not measured directly in order to avoid the thermal mass associated with contact thermometry.

As reported in Ref. 17, our PST displays a first-order ferroelectric phase transition at a Curie temperature of T_C ~ 295 K, consistent with a high degree of B-site cation order (~0.80). The field sweep rates for measuring $P_{\mathrm{iso}}(E)$ and $P_{\mathrm{adi}}(E)$ were identified by

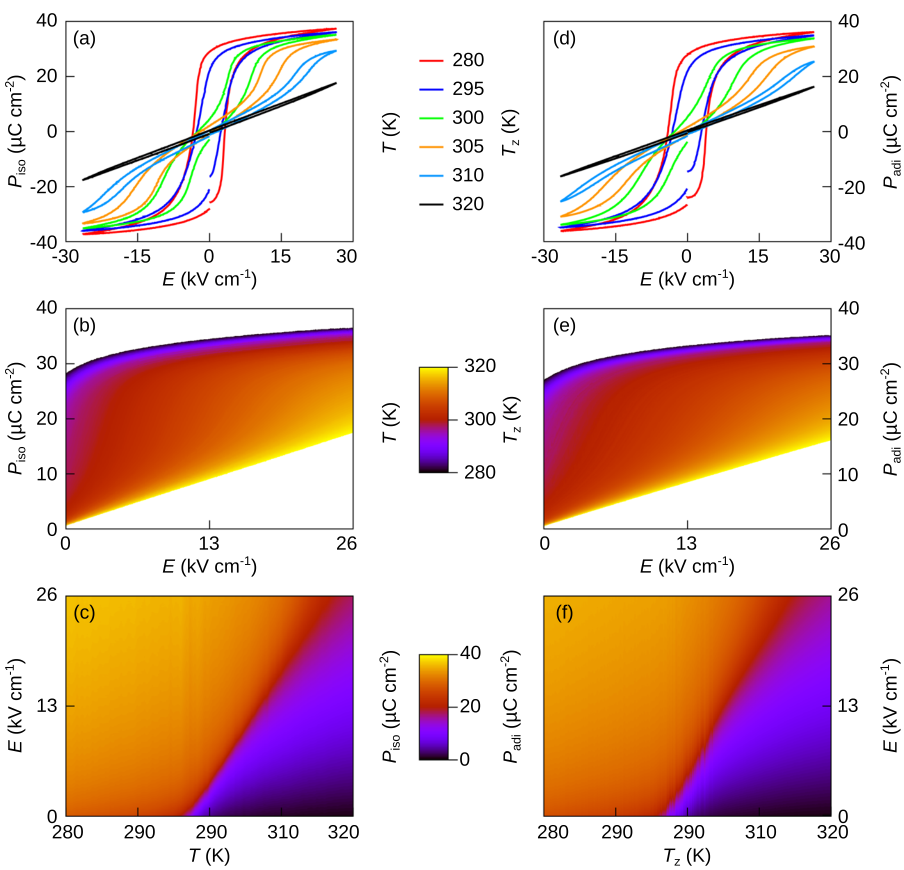

FIG. 1. Isothermal and adiabatic measurements of electrical polarization for a single sample of PST. [(a)–(c)] Isothermal bipolar $P_{\mathrm{iso}}(E)$ plots at 112 values of measurement temperature T every ~0.36 K are presented as (a) $P_{\mathrm{iso}}(E)$ for six values of T, (b) $T(E, P_{\mathrm{iso}})$ constructed from outer branches in $E \geq 0$ for all 112 values of T, and hence (c) $P_{\mathrm{iso}}(T, E)$. [(d)–(f)] Adiabatic bipolar $P_{\mathrm{adi}}(E)$ plots at 358 values of zero-field temperature T_z every ~0.11 K are presented as (d) $P_{\mathrm{adi}}(E)$ for six values of T_z, (e) $T_z(E, P_{\mathrm{adi}})$ constructed from outer branches in $E \geq 0$ for all 358 values of T_z, and hence (f) $P_{\mathrm{adi}}(E, T_z)$. Values of T_z were set on inner branches at $E = 0$ and represent the temperatures for the outer branches of interest at $E = 0$, assuming nominal reversibility. Note that adiabatic plots outnumber isothermal plots because equivalent warming runs permitted more fast field sweeps and fewer slow field sweeps.

comparing one quarter of the cycle period (during which the field varies between zero and its maximum value) with the thermal timescale, which was found to be ~5 s via direct EC measurements of a similarly mounted similar sample (see Note 4 of the supplementary material in Ref. 17), and which could be determined without direct EC measurements by employing ever more extreme periods until there is no change to $P_{iso}(E)$ and $P_{adi}(E)$. On heating slowly at 0.1 K min^{-1} from 280 K through T_C to 320 K, we obtained $P_{iso}(E)$ plots at 112 values of temperature T separated by ~0.36 K using the slow 30 s driving period to promote good thermalization while the field was varied [see Fig. 1(a) for six examples]. Plotting the outer branches in $E \geq 0$ for all 112 plots of $P_{iso}(E)$ yields Fig. 1(b). On repeating the temperature sweep, we obtained $P_{adi}(E)$ plots at 358 values of zero-field temperature T_z separated by ~0.11 K using the fast 0.5 s driving period to avoid any significant thermalization [see Fig. 1(d) for six examples]. Plotting the outer branches in $E \geq 0$ for all 358 plots of $P_{adi}(E)$ yields Fig. 1(e). By assuming that measurements of $P_{adi}(E)$ produce a nominally reversible adiabatic temperature change, we are able to assume that the zero-field temperature T_z prior to measurement is equal to the zero-field temperature on the outer branches of interest.

The individual plots of $P_{iso}(E)$ [Fig. 1(a)] and $P_{adi}(E)$ [Fig. 1(d)] evidence ferroelectricity below T_C, paraelectricity above T_C, and the electrically driven phase transition (double loop[17,25]) near and above T_C. The phase transition is hard to discern by eye when viewing the dense maps of polarization [Figs. 1(b) and 1(e)], but it can be clearly seen after the maps have been transposed onto E–T axes [Figs. 1(c) and 1(f)]. The gradient of the phase boundary is $|dE/dT_0|$ ~ 1 kV cm^{-1} K^{-1}, as expected for PST from the same master wafer[17] [transition temperature $T_0(E)$ equals T_C at $E = 0$].

Our quasi-indirect method can be understood from Fig. 2(a), where we have used white to copy the T_z = 305 K plot of $P_{adi}(E)$ from Fig. 1(d) and green to copy the 305 K and 307 K plots of $P_{iso}(E)$ from Fig. 1(b). Given that the plot of $P_{adi}(E)$ intersects the 305 K plot of $P_{iso}(E)$ at $E = 0$ and the 307 K plot of $P_{iso}(E)$ at our maximum applied field of E = 26 kV cm^{-1}, we infer that following the T_z = 305 K plot of $P_{adi}(E)$ from 0 to E = 26 kV cm^{-1} results in a nominally reversible adiabatic temperature change of $|\Delta T|$ ~ 307 K–305 K = 2 K with respect to T_z = 305 K.

Our quasi-indirect method can be implemented more generally to evaluate the values of $|\Delta T|$ for changes of field and starting temperatures that lie within our windows of isothermal and adiabatic measurement [Figs. 1(b) and 1(e)]. In Fig. 2(b), we reproduce from Fig. 1(b) all 112 plots of $P_{iso}(E)$ on a repeating color scale, whose 2 K period was chosen to match the value of $|\Delta T|$ that we identified above. Overlaid in white, we reproduce from Fig. 1(e) some of the 358 plots of $P_{adi}(E)$. Specifically, we show relatively well-spaced plots of $P_{adi}(E)$ for intermediate values of T_z that differ by ~2 K. Conceptually, one should imagine all 358 plots of $P_{adi}(E)$ to be present, but, of course, we cannot show them all without masking the colorful $P_{iso}(E)$ plots. These colorful plots represent a temperature map, and they have inspired us to call this paper the "rainbow paper."

One can evaluate $|\Delta T|$ by eye when following a white $P_{adi}(E)$ plot between start and end points that lie around the middle of Fig. 2(b) such that each of these points can be identified with two specific $P_{iso}(E)$ plots that are identified by color. Suppose that a starting field and a starting temperature correspond to a specific point on a $P_{iso}(E)$ plot that is red. One should then identify the intersecting white plot of $P_{adi}(E)$, which might or might not be one of the 358 $P_{adi}(E)$ plots that we happen to show. One follows the intersecting white plot of $P_{adi}(E)$ up to the finishing field and evaluates $|\Delta T|$ via the color change associated with the intersecting plots of $P_{iso}(E)$. For example, if one were to follow a white plot from one red contour to the next, then one would have completed one period, implying $|\Delta T|$ = 2 K. Inspection of both Figs. 2(a) and 2(b) indicates that a temperature change of this magnitude might just be possible.

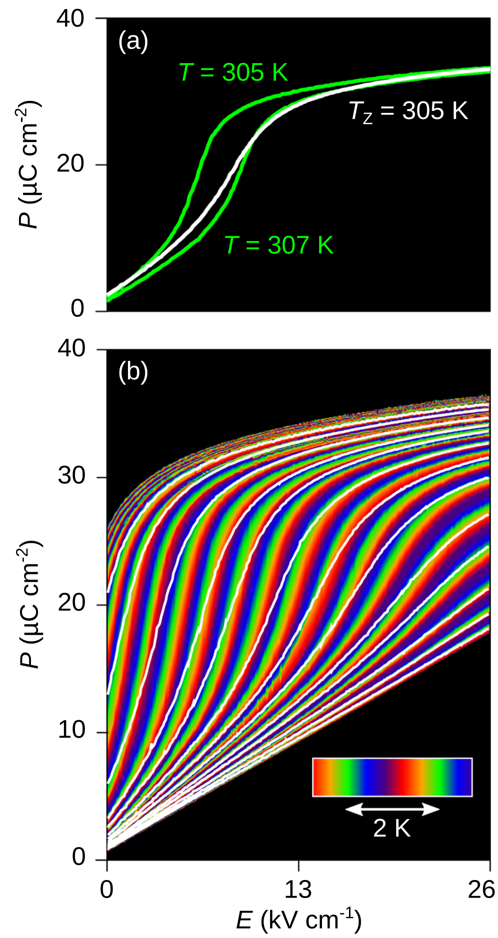

FIG. 2. Comparison of the isothermal and adiabatic electrical polarization data in Fig. 1. Data are presented for outer branches in $E \geq 0$. (a) $P_{adi}(E)$ for T_z = 305 K (white) and $P_{iso}(E)$ at 305 K (upper green plot) and 307 K (lower green plot). (b) $P_{adi}(E)$ for a subset of T_z values every ~2 K in the middle part of the measurement range such that 280 K $\ll T_z \ll$ 320 K (white plots) and $P_{iso}(E)$ for all T values every ~0.36 K in 280 K $\leq T_z \leq$ 320 K (periodic color scale). The temperature for a given $P_{iso}(E)$ plot may be identified by counting repeats of the color scale with respect to the lowest-lying isotherm at 320 K. Note that all values of $P_{adi}(E)$ were scaled up by 3.1% to match $P_{iso}(E)$ below T_C, where EC effects are negligible.[17] This scaling corrects a systematic error in the saturation polarizations that we identified when using a frequency-dependent input impedance to measure very different displacement currents on very different timescales.

Visual evaluation becomes unreliable when the colorful plots of $P_{iso}(E)$ are closely bunched, but the values of $|\Delta T|$ can nevertheless be established by computation, and accuracy can be improved by averaging over similar trajectories (see Note 1 of the supplementary material). Using this method, we plot $|\Delta T(T_z)|$ [Fig. 3(a)] for a field change that approximately corresponds to our maximum field change from 0 kV cm^{-1} to 26 kV cm^{-1}, and we find a maximum value of $|\Delta T| \sim 1.7 \pm 0.2$ K in 300 K < T_z < 315 K. Using a statistical method (see Note 2 of the supplementary material) yielded a similar plot of $|\Delta T(T_z)|$ [Fig. 3(b)], again with a maximum value of $|\Delta T| \sim 1.7 \pm 0.2$ K in 300 K < T_z < 315 K, but without the spurious large values of $|\Delta T(T_z)|$ at low and high temperatures [data shown with dark gray error bars in Fig. 3(a)].

Our maximum temperature change of ~1.7 ± 0.2 K occurs in a range of temperatures that is similar with respect to our data for PST from the same wafer,[17] but our peak value is slightly smaller than the directly measured value of $|\Delta T| \sim 2.2$ K (which is itself slightly smaller than the indirectly measured value[17]). Let us now consider the origin of this discrepancy. The $P_{adi}(E)$ data were adiabatic because each branch was measured over 0.125 s (one quarter of the 0.5 s period), which is 40 times faster than the ~5 s thermal timescale for exponential decay. However, the $P_{iso}(E)$ data were not properly isothermal because each branch was measured over 7.5 s (one quarter of the 30 s period that represents an upper bound imposed by the proprietary software of the Radiant ferroelectric tester), which is only slightly greater than the ~5 s thermal timescale for exponential decay. This discrepancy with respect to isothermal conditions leads to the conservative values of $|\Delta T|$, but it is difficult to quantify the error, partly because the first-order phase transition is locally discontinuous, and partly because heat will be exchanged within the thus phase-separated sample. In future work, one should ensure that $P_{iso}(E)$ is isothermal throughout by varying the applied field sufficiently slowly, e.g., using the constant-current method with a sufficiently low current.[18,26,27] Separately, one should ensure that the measurement temperature is swept slowly enough to measure $P_{iso}(E)$ at temperatures whose separation is as small as possible a fraction of $|\Delta T|$.

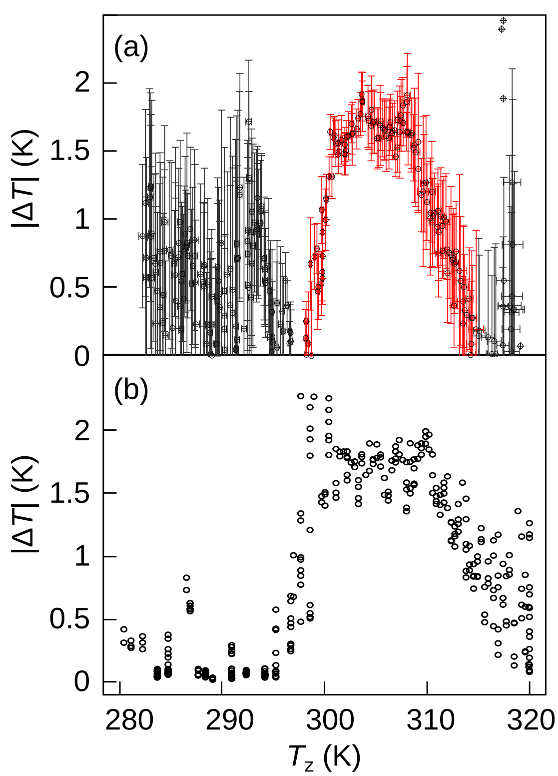

FIG. 3. Summary of adiabatic temperature change. Plots of $|\Delta T(T_z)|$ were identified for a change of field between 0 and ~26 kV cm^{-1} using (a) linear interpolation (see Note 1 of the supplementary material) and (b) statistical analysis (see Note 2 of the supplementary material). Data shown with dark gray error bars in (a) represent false positive outcomes of the method.

In summary, the quasi-indirect method involves following a rapidly acquired plot of adiabatic polarization vs field and identifying the EC temperature change by reading the temperatures of the isothermal plots that it crosses. Although the thermometer in the cryogenic probe is used to identify starting (measurement) temperatures for the adiabatic (isothermal) plots, it does not measure EC temperature change, permitting one to regard the sample as if it were itself a thermometer. In this respect, the quasi-indirect method differs from the direct, indirect, and quasi-direct methods and may provide an attractive alternative in circumstances where these other methods prove challenging. One exciting possibility is to use the quasi-indirect method to measure free-standing EC films. For example, one might hope to measure films that are tens of micrometers thick at hundreds of kilohertz (10-fold thickness reduction with respect to the present sample implies 100-fold reduction in thermalization time[24]). One might also use modeling to back out adiabatic limits that cannot be reached in practice.

See the supplementary material for the evaluation of $|\Delta T|$ using first linear interpolation and averaging (Note 1) and then a statistical method (Note 2).

We thank P. C. Osbond for fabricating the master sample. We thank EPSRC (UK) for funding under Grant No. EP/M003752/1. X.M. is grateful for support from the Royal Society under Grant No. URF\R\180035.

DATA AVAILABILITY

The data that support the findings of this study are available within the article and its supplementary material.

REFERENCES

[1] X. Moya, S. Kar-Narayan, and N. D. Mathur, Nat. Mater. **13**, 439 (2014).
[2] X. Moya and N. D. Mathur, Science **370**, 797 (2020).
[3] Y. V. Sinyavsky, N. D. Pashkov, Y. M. Gorovoy, G. E. Lugansky, and L. Shebanov, Ferroelectrics **90**, 213 (1989).
[4] Y. V. Sinyavsky and V. M. Brodyansky, Ferroelectrics **131**, 321 (1992).
[5] Y. V. Sinyavskii, Chem. Petrol. Eng. **31**, 295 (1995).
[6] U. Plaznik, A. Kitanovski, B. Rožič, B. Malič, H. Uršič, S. Drnovšek, J. Cilenšek, M. Vrabelj, A. Poredoš, and Z. Kutnjak, Appl. Phys. Lett. **106**, 043903 (2015).
[7] Y. Jia and Y. Sungtaek Ju, Appl. Phys. Lett. **100**, 242901 (2012).
[8] H. Gu, X. Qian, X. Li, B. Craven, W. Zhu, A. Cheng, S. C. Yao, and Q. M. Zhang, Appl. Phys. Lett. **102**, 122904 (2013).
[9] Y. D. Wang, S. J. Smullin, M. J. Sheridan, Q. Wang, C. Eldershaw, and D. E. Schwartz, Appl. Phys. Lett. **107**, 134103 (2015).
[10] D. Sette, A. Asseman, M. Gérard, H. Strozyk, R. Faye, and E. Defay, APL Mater. **4**, 091101 (2016).

[11] P. Blumenthal, C. Molin, S. Gebhardt, and A. Raatz, Ferroelectrics **497**, 1 (2016).
[12] T. Zhang, X.-S. Qian, H. Gu, Y. Hou, and Q. M. Zhang, Appl. Phys. Lett. **110**, 243503 (2017).
[13] R. Ma, Z. Zhang, K. Tong, D. Huber, R. Kornbluh, Y. S. Ju, and Q. Pei, Science **357**, 1130 (2017).
[14] A. Torelló, P. Lheritier, T. Usui, Y. Nouchokgwe, M. Gérard, O. Bouton, S. Hirose, and E. Defay, Science **370**, 125 (2020).
[15] Y. Wang, Z. Zhang, T. Usui, M. Benedict, S. Hirose, J. Lee, J. Kalb, and D. Schwartz, Science **370**, 129 (2020).
[16] Y. Meng, Z. Zhang, H. Wu, R. Wu, J. Wu, H. Wang, and Q. Pei, Nat. Energy **5**, 996 (2020).
[17] S. Crossley, B. Nair, R. W. Whatmore, X. Moya, and N. D. Mathur, Phys. Rev. X **9**, 041002 (2019).
[18] B. Nair, T. Usui, S. Crossley, S. Kurdi, G. G. Guzmán-Verri, X. Moya, S. Hirose, and N. D. Mathur, Nature **575**, 468 (2019).
[19] B. Nair, Ph.D. thesis, University of Cambridge, 2020, available at https://www.repository.cam.ac.uk/handle/1810/312805.
[20] R. Z. Levitin, V. V. Snegirev, A. V. Kopylov, A. S. Lagutin, and A. Gerber, J. Magn. Magn. Mater. **170**, 223 (1997).
[21] X. Moya, E. Stern-Taulats, S. Crossley, D. González-Alonso, S. Kar-Narayan, A. Planes, L. Mañosa, and N. D. Mathur, Adv. Mater. **25**, 1360 (2013).
[22] Y. Bai, K. Ding, G.-P. Zheng, S.-Q. Shi, and L. Qiao, Phys. Status Solidi A **209**, 941 (2012).
[23] C. H. Séquin, Solid-State Electron. **14**, 417 (1970).
[24] S. Crossley, Ph.D. thesis, University of Cambridge, 2013, available at http://www.repository.cam.ac.uk/handle/1810/245063.
[25] W. J. Merz, Phys. Rev. **91**, 513 (1953).
[26] J. A. Giacometti, C. Wisniewski, W. A. Moura, and P. A. Ribeiro, Rev. Sci. Instrum. **70**, 2699 (1999).
[27] D.-Y. Wang and C.-Y. Chang, Jpn. J. Appl. Phys., Part 1 **43**, 4263 (2004).